Improved Monte Carlo Localization for Agricultural Mobile Robots with the Normal Distributions Transform

Brian Lai Lap Hong, Mohd Azri Bin Mohd Izhar, Norulhusna Binti Ahmad
Faculty of Artificial Intelligence, Universiti Teknologi Malaysia, Kuala Lumpur, Malaysia

***Abstract*—Localization is crucial for robots to navigate autonomously in agricultural environments. This paper introduces an improved Adaptive Monte Carlo Localization (AMCL) algorithm integrated with the Normal Distributions Transform (NDT) to address the challenges of navigation in agricultural fields. 2D Light Detection and Ranging (LiDAR) measures distances to surrounding objects using laser light, and captures distance data in a single horizontal plane, making it ideal for detecting obstacles and field features such as trees and crop rows. While conventional AMCL has been studied for indoor environments, there is a lack of research on its application in outdoor agricultural settings, particularly when using 2D LiDAR. The proposed method enhances localization accuracy by applying the NDT after the conventional AMCL estimation, refining the pose estimate through a more detailed alignment of the 2D LiDAR data with the map. Simulations conducted in a palm oil plantation environment demonstrate a 53% reduction in absolute pose error and a 50% reduction in relative position error compared to conventional AMCL. This highlights the potential of the AMCL-NDT approach with 2D LiDAR for cost-effective and scalable deployment in precision agriculture.**

***Keywords*—Adaptive Monte Carlo Localization; Normal Distributions Transform; pose estimation; precision agriculture; agricultural robotics; outdoor localization**

I. Introduction

Localization is fundamental for autonomous robotics, especially in outdoor environments like agriculture. The current trend in smart agriculture, known as Precision Agriculture (PA), involves robotic for tasks such as planting, monitoring, and harvesting [1], [2]. These tasks rely on accurate localization to navigate through fields, perform targeted actions, and adapt to varying environmental conditions. However, outdoor environments introduce challenges such as environmental variability, dynamic obstacles, and sparse or repetitive features, which complicate localization [3], [4].

The foundation for autonomous navigation localization which is required to perform navigation tasks such as mapping, path planning, and obstacle avoidance. One of the most widely used probabilistic localization techniques is Adaptive Monte Carlo Localization (AMCL), which leverages particle filters to estimate a robot's pose relative to a known map [5]. AMCL has proven effective in structured indoor environments due to its reliance on well-defined features and low sensor noise. However, in outdoor, unstructured environments such as agricultural fields, the application of AMCL is limited by challenges such as sparse features, dynamic obstacles, and environmental variability [4], [6], [7].

Agricultural environments often have recurring patterns, such as rows of crops, which can confuse conventional localization algorithms by introducing uncertainties in pose estimation [3]. Additionally, uneven and scattered attributes like tree trunks or uneven terrain complicate the localization process [8]. Finally, dynamic elements, such as moving branches and changing lighting conditions, introduce further noise, reducing the reliability of traditional AMCL [9].

Light Detection and Ranging (LiDAR) is widely employed in robotics for measuring distances through laser beam emission and reflection analysis. It generates high-resolution 2D maps or point clouds representing environmental surfaces, offering essential data for localization and mapping. 2D LiDAR sensors are cost-effective and computationally efficient. However, their limited data often hinder robust localization, particularly in outdoor settings [10].

Despite its widespread application in robotics, AMCL exhibits several limitations when applied to 2D LiDAR in outdoor environments. AMCL is designed for indoor environments which are distinctive and consistent [6], [11]. In contrast, outdoor agricultural environments often lack such features which can lead to significant localization errors [8], [12]. Additionally, AMCL relies heavily on distinctive features to estimate pose estimates, and its performance highly affected in feature-sparse areas, causing drift and uncertainty [13], [14]. AMCL also struggles in symmetrical environments, as it may incorrectly converge to an equivalent but incorrect pose due to the lack of unique landmarks [6]. Furthermore, existing research predominantly focuses on improving AMCL in controlled indoor environments, with limited attention given to its adaptation and optimization for dynamic and unstructured outdoor agricultural scenarios [11], [12].

To address these challenges, researchers have experimented with scan matching algorithms, such as Iterative Closest Point (ICP) and the Normal Distributions Transform (NDT), which refine pose estimates by aligning sensor data with reference maps [15]–[17]. These methods do improve the accuracy of localization, particularly in environments with sparse or ambiguous features. However, these studies focus solely on scan matching and do not integrate these methods with AMCL, which limits their ability to maintain the probabilistic framework needed for effective localization in dynamic environments. Furthermore, implementing scan matching algorithms in agricultural fields, which are normally large in size, introduces scalability issues due to their computational demands [18].

This paper proposes an improved localization algorithm that integrates AMCL and the NDT, specifically for outdoor agricultural environments. By enhancing AMCL with the NDT, the proposed method addresses the limitations of conventional AMCL in unstructured and repetitive layouts. The result will be evaluated with Absolute Pose Error (APE) and Relative Pose Error (RPE) which will be further explained in Section III. The contributions of this work include:

- A localization approach combining AMCL with NDT for robotics in an agricultural environment.
- Benchmarking results against conventional AMCL with APE and RPE, highlighting significant improvements in localization accuracy.

The remainder of this paper is structured as follows: Section II (AMCL Algorithm) provides a detailed explanation of the AMCL algorithm and its limitations in agricultural environments. Section III (Proposed Methodology) describes the proposed methodology, outlining the integration of AMCL with NDT and the experimental setup used for validation. Section IV (Results) presents the results, comparing the performance of conventional AMCL and the proposed AMCL-NDT hybrid using APE and RPE metrics. Section V (Discussion) analyzes the findings, discussing the trade-offs and practical implications of the proposed approach. Finally, Section VI (Conclusion) summarizes the key takeaways and suggests future research directions.

II. AMCL Algorithm

AMCL is a probabilistic algorithm that utilizes particle filters to estimate a robot's pose (position and orientation) within a known environment. By integrating sensory data such as 2D LiDAR and odometry with a pre-built map, AMCL achieves precise localization accuracy.

AMCL represents the robot's belief about its location using a set of particles. Each particle, p, corresponds to a potential pose of the robot and is assigned a weight, w, reflecting the likelihood of that pose being correct.

At each time step k, the algorithm updates the state of each particle p based on the robot's motion, incorporating odometry data u. This step accounts for uncertainties introduced by motion errors such as wheel slippage or uneven terrain.

Each particle's weight w is updated by comparing the predicted pose to sensor data z. This weighting step measures how well the particle's pose matches the actual sensor reading, typically coming from a 2D LiDAR.

After the particles have been updated, the particles with higher weights are retained and replicated, while particles with lower weights are discarded. This ensures that the particle set focuses more on likely robot poses. The resampling step produces a new set of particles P', which is then set as the current particle set P.

The robot's estimated pose at time step k, denoted $\hat{x}_k$, is computed as the weighted average of all the particles. This provides a probabilistic estimate of the robot's location based on the particle set.

AMCL dynamically adjusts the number of particles N depending on the uncertainty of the robot's location. In areas with high uncertainty, N is increased to improve accuracy. In more constrained areas, N is reduced to optimize computational efficiency. This algorithm can be further shown in Algorithm 1.

Algorithm 1 AMCL Algorithm

Input: initial pose estimate $\mathbf{x_0}$ (if available from step 18)
Initialize particles $P = \{p_1, p_2, \ldots, p_N\}$
Initialize weights $W = \{w_1, w_2, \ldots, w_N\}$
Set $k = 0$ {Time step}
Initialize last pose $\hat{x}_{k-1}$ as an estimate of the robot's initial pose (if available from step 18)
while robot is active **do**
  $k \leftarrow k + 1$
  $u_k \leftarrow$ control input {Motion command}
  $z_k \leftarrow$ observation {Sensor reading}
  for each particle $p_i \in P$ **do**
    $p_i \leftarrow \text{motion}(p_i, u_k, \hat{x}_{k-1})$ {Feedback: Update particle state based on last pose}
    $w_i \leftarrow \text{measurement}(p_i, z_k)$
  end for
  Normalize weights:

$$w_i \leftarrow \frac{w_i}{\sum_{j=1}^{N} w_j}$$

  Resample particles based on weights W to form new particles P' {Feedback: Resample based on particle weights}
  Set $P \leftarrow P'$ {Update particle set with new resampled particles}
  Estimate robot pose using weighted particles:

$$\hat{x}_k \leftarrow \sum_{i=1}^{N} w_i p_i$$

  Set $\hat{x}_{k-1} \leftarrow \hat{x}_k$ {Update last pose for next iteration}
end while

III. Proposed Methodology

The objective of this research is to improve the accuracy of localization in agricultural environments, specifically in palm oil plantations, by integrating Adaptive Monte Carlo Localization (AMCL) with Normal Distributions Transform (NDT). AMCL is used to provide an initial estimate of the robot's pose, and NDT is applied to refine this estimate by aligning the robot's LiDAR scans with a reference map of the environment. This two-pronged approach aims to enhance robot navigation in repetitive and sparse environments, which is a common challenge in agricultural settings. To simulate the agricultural environment, we use Gazebo, a popular robotics simulation platform, which replicates an outdoor farm environment modeled after a palm oil plantation. This simulation is grounded in real-world data we collected from an actual palm oil plantation in Malaysia. The layout of the plantation, including terrain features, paths, and obstacles, was accurately captured to ensure that the simulation reflects real-world conditions. For localization, we utilize a Portable Gray Map (PGM) that was generated via Simultaneous Localization and Mapping

(SLAM). This map serves as the reference map against which the robot's position will be estimated. The map is voxelized, meaning it is represented as a grid of discrete cells, each containing statistical information about the environment, which helps the robot localize itself based on sensor data.

A. AMCL and NDT Integration

The core of the proposed methodology involves using AMCL to estimate the robot's initial pose, denoted as $\mathbf{x_0}$, through a particle filter. This initial pose is then refined using the NDT algorithm. The NDT algorithm works by aligning the robot's LiDAR scan, denoted as $\mathbf{S}$, with the reference map $\mathbf{M}$, which has been voxelized. The algorithm treats the map as a collection of NDT cells, where each cell represents a normal distribution of points in 3D space. The NDT minimizes the error between the scan and the map by iteratively optimizing the robot's pose. This process is essential in environments where AMCL alone might struggle due to repetitive features or sparse data.

1) Step 1: Initial pose estimation with AMCL: The first step in the localization process is to use AMCL to estimate the robot's initial pose. AMCL works by using a particle filter technique, which probabilistically estimates the robot's position based on motion commands and sensor measurements (i.e., LiDAR scans). The particle filter generates a set of particles, each representing a potential pose, and weights them based on how well the sensor data matches the map. The pose corresponding to the highest-weighted particle is taken as the initial estimate of the robot's location, denoted as $\mathbf{x_0}$. In the context of this research, AMCL is applied to the robot's scan $\mathbf{S}$ and the map $\mathbf{M}$ obtained from the SLAM process. This initial pose estimate provides a starting point for the next step, which involves the refinement of this estimate using NDT.

2) Step 2: Pose refinement with NDT: Once the AMCL algorithm provides an initial pose estimate $\mathbf{x_0}$, the NDT algorithm is used to refine this estimate. The NDT algorithm works by aligning the robot's LiDAR scan $\mathbf{S}$ with the reference map $\mathbf{M}$, which has been voxelized. The algorithm treats the map as a collection of NDT cells, where each cell represents a normal distribution of points in 3D space. These NDT cells are compared to the robot's current LiDAR scan to find the best alignment between the scan and the map. The goal of NDT is to minimize the error between the scan and the map by iteratively optimizing the robot's pose. This is done by calculating the likelihood of the scan points fitting into the NDT cells in the map, and updating the pose estimate $\mathbf{x}$ through an optimization process that uses a gradient descent method.

The process begins by transforming the scan $\mathbf{S}$ according to the current pose estimate $\mathbf{x}$, resulting in a transformed scan $\mathbf{S}_T$. This transformed scan is then compared against the reference map $\mathbf{M}$, and the likelihood of each scan point fitting within the NDT cells of the map is computed. Based on this comparison, the pose estimate $\mathbf{x}$ is updated by calculating the gradient of the error term $\mathbf{e}$, which quantifies the difference between the transformed scan $\mathbf{S}_T$ and the map $\mathbf{M}$.

3) Step 3: Pose optimization and feedback: After NDT has refined the pose estimate, the optimized pose $\mathbf{x}^*$ is used to update the AMCL algorithm for the next cycle of localization. This feedback loop is essential, as it allows AMCL to incorporate the more accurate pose information from NDT to adjust its particle filter. As a result, AMCL's subsequent estimates are more precise, and the localization process becomes more robust over time. The feedback mechanism operates in a way that, after each NDT optimization, the refined pose is used to update the initial guess $\mathbf{x_0}$ for AMCL. This iterative refinement leads to a continuous improvement in localization accuracy, especially in environments that may have repetitive patterns or sparse features that make traditional AMCL less effective (Fig. 1).

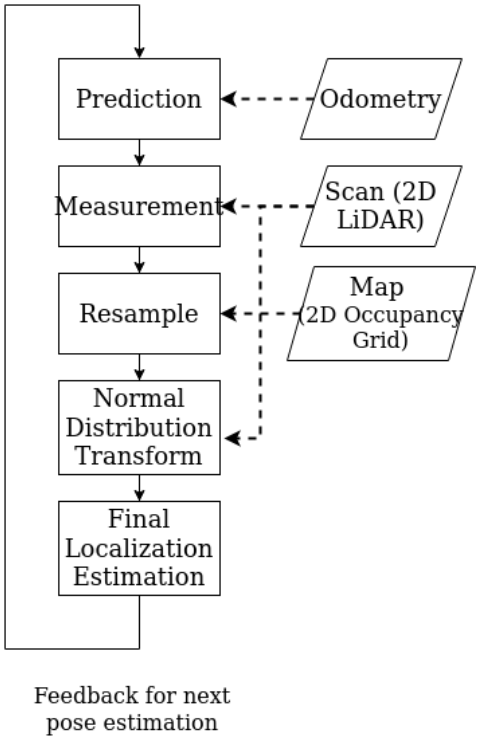

Fig. 1. Flow chart of AMCL with NDT.

B. Algorithm Explanation (NDT)

The following algorithm outlines the NDT process that refines the initial pose estimate obtained from AMCL:

C. Performance Evaluation

To evaluate the performance of the proposed methods, two key metrics were used: APE and RPE, as defined in [19].

1) Absolute pose error: The precise discrepancies between a robot's perceived location (estimated pose) and its real location (ground truth) at particular moments are computed via the absolute pose error. The APE is calculated as follows:

$$APE = G_i^{-1} S P_i \tag{1}$$

where G_i represents the ground truth pose at time i, P_i represents the estimated pose, and S is the rigid-body transformation that aligns the estimated trajectory to the ground truth using a least-squares solution [20].

Algorithm 2 Normal Distributions Transform (NDT)

Input: Initial scan $\mathbf{S}$, map $\mathbf{M}$, initial pose estimate $\mathbf{x_0}$
Output: Optimized pose $\mathbf{x}^*$
Initialize $\mathbf{x} \leftarrow \mathbf{x_0}$ {Initial pose estimate}
Convert the map $\mathbf{M}$ into NDT cells (representing normal distributions)
for iteration = 1 to max_iterations **do**
  Transform the scan $\mathbf{S}$ according to current pose $\mathbf{x}$, resulting in $\mathbf{S}_T$
  Compute NDT cells for the transformed scan $\mathbf{S}_T$
  For each NDT cell in the map:
  for each point in transformed scan $\mathbf{S}_T$ **do**
    Find closest NDT cell in the map
    Compute likelihood of the scan point fitting the NDT cell's distribution
  end for
  Compute error term $\mathbf{e}$ based on scan fitting in NDT cells
  Compute gradient of error term with respect to the pose $\mathbf{x}$
  Update the pose: $\mathbf{x} \leftarrow \mathbf{x} - \alpha \cdot \nabla_{\mathbf{x}}\mathbf{e}$
  if convergence criteria satisfied **then**
    break
  end if
end for
Return optimized pose $\mathbf{x}^*$

2) Relative pose error: Instead of determining the robot's precise location at a given moment in time, the relative pose error computes the variations in its movement over a predetermined distance or period.:

$$RPE = (G_i^{-1}G_{i-\Delta})(P_i^{-1}P_{i-\Delta}) \tag{2}$$

where Δ represents the time interval over which the relative poses are computed. The RPE can be computed for both translational and rotational components.

Both APE and RPE are evaluated using the Root Mean Squared Error (RMSE), as defined below:

$$RMSE_{APE} = \frac{1}{n}\sum_{n}^{i=1}(\|trans(APE_i)\|^2)^{\frac{1}{2}} \tag{3}$$

$$RMSE_{(RPE,\Delta)} = \frac{1}{n}\sum_{n}^{i=1}(\|trans(RPE_i)\|^2)^{\frac{1}{2}} \tag{4}$$

where $trans(APE_i)$ and $trans(RPE_i)$ refer to the translational components of the APE and RPE.

D. Experimental Setup

The setup of the Gazebo simulation is generated with PGM derived from an actual palm oil field. The setup involves the following tools and platform:

Table I show the overall setup for the simulation. The experiment setup uses the Ubuntu Jammy Jellyfish 22.04 operating system with ROS 2 Humble Hawksbill. The robot model used in this experiment is the Clearpath Husky, which is equipped with a Hokuyo UTM-30LX LIDAR sensor. The PGM image size is 2535 × 2014 pixels. The map size of the environment is 126.75 meters by 100 meters, representing the palm oil field. The tree trunk diameter in the simulation is set to 1.5 meters. Fig. 2 shows the sample of the image that has been generated using PGM, and Fig. 3 shows the simulation environment in the Gazebo software.

TABLE I. TOOLS AND PLATFORM

Operating System	Ubuntu Jammy Jellyfish 22.04
ROS version	ROS 2 Humble Hawksbill
Robot model	Clearpath Husky
LIDAR	Hokuyo UTM-30LX
Image size(pixel)	2535 × 2014
Map size(mete)	26.75 x 100
Tree trunk diameter(metre)	1.5

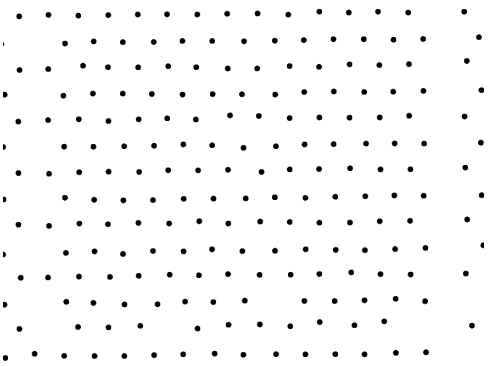

Fig. 2. A PGM map generated based on palm oil plantation and each dot represent a tree.

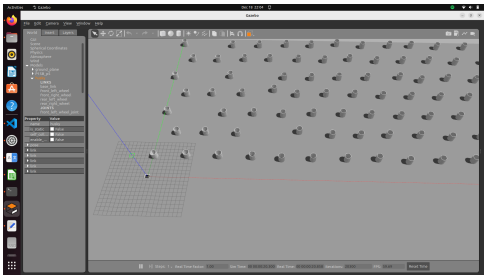

Fig. 3. Gazebo simulation based on PGM and each cylinder represent a tree.

E. Simulation Environment Parameters

1) Simulation parameters for AMCL: AMCL setup is configured with specific parameters: the minimum angular update is set to 0.5, and the minimum distance update is set to 0.2. The algorithm's alpha values, which represent the process noise, are set to 0.2 for all four parameters, as described in Table II.

TABLE II. AMCL ALPHA PARAMETER DESCRIPTIONS

Alpha Parameter	Description
alpha1	Expected process noise in odometry's rotation estimate from rotation.
alpha2	Expected process noise in odometry's rotation estimate from translation.
alpha3	Expected process noise in odometry's translation estimate from translation.
alpha4	Expected process noise in odometry's translation estimate from rotation.

2) Simulation parameters for the NDT: In the simulation for NDT, several key parameters are configured to control the optimization and registration process. The Euclidean fitness score is used to determine the threshold for an acceptable alignment between point clouds. NDT step size controls the magnitude of transformation adjustments in each iteration. NDT resolution defines the size of the grid cells used in the transformation process, affecting the level of detail in the NDT grid representation. Transformation epsilon ensures that the algorithm halts when small changes in the transformation are no longer significant.

The simulation for the NDT uses these parameters namely Euclidean fitness score of 2.0, the NDT step size of 0.1, and the NDT resolution of 2.0. The transformation epsilon is set to 0.01, ensuring that small changes in the transformation are considered. Additionally, the use of IMU and odometry data is disabled in this simulation, as these sensors are not required for the current setup.

IV. RESULTS

This study compares the localization performance of AMCL and the proposed AMCL with NDT hybrid method using two primary metrics: APE and RPE. The comparison is summarized in Table III.

TABLE III. COMPARISON OF AMCL AND THE NDT BASED ON PERFORMANCE METRIC

Result [m]	APE		RPE	
	AMCL	**AMCL with NDT**	**AMCL**	**AMCL with NDT**
Max	0.70	1.12	4.94	4.80
Mean	0.41	0.49	1.12	0.15
Median	0.43	0.48	0.91	0.08
Min	0.01	0.04	0.00	0.00
RMSE	0.43	0.52	1.46	0.41
SSE	215.83	320.23	2630.72	50.27
Std Dev, σ	0.11	0.17	0.95	0.38

In this section, we present a detailed comparison of the performance of the AMCL and AMCL with NDT based on both APE and RPE. The results for both metrics are summarized in Table III.

A. APE Comparison

AMCL with NDT demonstrates slight improvements in certain APE metrics compared to AMCL. While the maximum APE for AMCL with NDT (1.12 m) is 60% higher than for AMCL (0.70 m), the mean APE for AMCL with NDT (0.49 m) is only slightly higher than AMCL (0.41 m), with a 19.51% increase. The median APE for AMCL with NDT (0.48 m) is also slightly higher (11.63% increase) than for AMCL (0.43 m). The minimum APE for AMCL with NDT is 300% higher than for AMCL, though the methods perform similarly in ideal conditions (0.04 m vs. 0.01 m).

Despite these minor increases in APE, AMCL with NDT shows improved robustness and consistency, especially in more complex scenarios. The RMSE for AMCL with NDT is 0.52 m, 20.93% higher than for AMCL, and the SSE is also higher for AMCL with NDT (320.23 vs. 215.83), which indicates greater error accumulation. However, AMCL with NDT's higher standard deviation, σ, (0.17 vs. 0.11) reflects the added complexity introduced by the NDT, though it still offers a more stable solution in real-world applications.

B. RPE Comparison

AMCL with NDT significantly outperforms AMCL in all RPE metrics, particularly in terms of reducing relative pose estimation errors. The maximum RPE for AMCL with NDT (4.80 m) is 2.83% lower than for AMCL (4.94 m). More notably, the mean RPE for AMCL with NDT is 86.61% lower (0.15 m vs. 1.12 m), and the median RPE is 91.21% lower (0.08 m vs. 0.91 m), highlighting the superior accuracy of AMCL with NDT in relative pose estimation.

AMCL with NDT also outperforms AMCL in terms of RMSE, with a 71.23% reduction (0.41 m vs. 1.46 m), and a dramatic decrease in SSE (50.27 vs. 2630.72), which shows a much lower error accumulation. The standard deviation, σ, of AMCL with NDT (0.38) is 60% lower than AMCL (0.95), indicating better consistency across various conditions. These results demonstrate that AMCL with NDT provides a much more reliable and accurate localization solution for relative pose estimation, making it the preferable method when accuracy and consistency are prioritized.

C. Trajectory Comparison

This section compares the localization performance of AMCL and AMCL with NDT using APE and RPE metrics based on the provided trajectory error maps in Fig. 4 and Fig. 5 using the conventional AMCL algorithm and the proposed AMCL with NDT algorithm, respectively.

1) APE Comparison: The map showing the trajectory with color visualization of APE for AMCL with NDT, as shown in Fig. 5(a), illustrates excellent trajectory alignment with the reference path. Most of the trajectory is dominated by blue and green shades, signifying minimal deviation, with rare occurrences of higher-error regions. This underscores its accuracy and reliability.

The map showing the trajectory with color visualization of APE for AMCL, as shown in Fig. 4(a), reveals more distributed yellow and red patches, especially in curved and looped sections of the trajectory. These regions highlight AMCL's difficulty in maintaining consistent alignment with the reference trajectory.

AMCL with NDT demonstrates superior performance with significantly lower APE, providing better alignment with the reference trajectory compared to AMCL, which shows limitations in accuracy and stability in more complex trajectory sections.

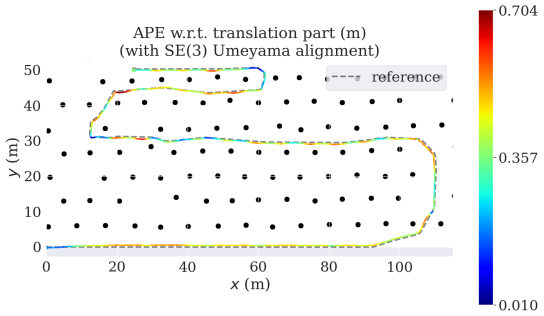

(a) APE.

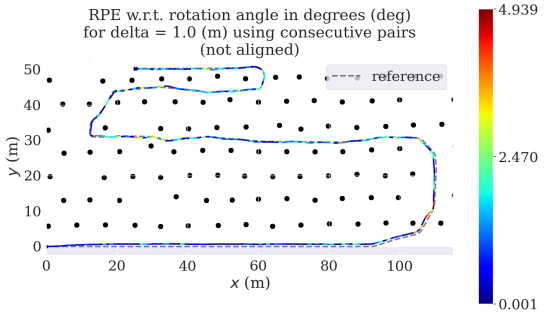

(b) RPE.

Fig. 4. Comparison of trajectories between the conventional AMCL algorithm and ground truth with visualization of APE and RPE.

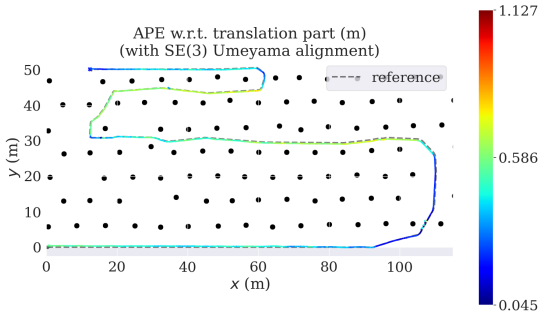

(a) APE.

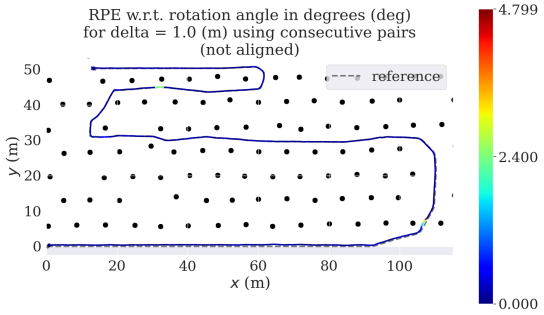

(b) RPE.

Fig. 5. Comparison of trajectories between the proposed AMCL with NDT algorithm and ground truth with visualization of APE and RPE.

2) RPE Comparison: The trajectory with color visualization of RPE for AMCL with NDT, as shown in Fig. 5(b), demonstrates consistently low errors. Most of the trajectory is represented in blue and green shades, indicating minimal deviations, with occasional yellow or red areas observed in dynamic sections. This highlights the robustness of AMCL with NDT in pose estimation, even during transitions or sharp turns.

In comparison, the map showing the trajectory with color visualization of RPE for AMCL, as shown in Fig. 4(b), shows higher error regions. The trajectory contains more frequent yellow and red shades, particularly in areas involving sharp turns or trajectory loops, suggesting greater susceptibility to drift and motion dynamics.

Overall, AMCL with NDT outperforms AMCL by maintaining consistently lower RPE, ensuring stable localization across the trajectory. AMCL, on the other hand, shows higher error variability in dynamic scenarios.

V. Discussion

The results presented in the previous section highlight the advantages of integrating the AMCL algorithm with NDT in agricultural robotics. While AMCL with NDT introduces a slight increase in APE, especially in the maximum APE value, it significantly improves the RPE, reducing both mean and RMSE values by substantial margins. These improvements in RPE are especially important for agricultural applications where relative pose accuracy is critical for navigating large-scale fields and avoiding obstacles.

The increased complexity introduced by NDT, reflected in the higher standard deviation and SSE, is a trade-off for the superior accuracy in relative pose estimation. The AMCL with NDT hybrid approach provides a more consistent and stable localization solution, especially in complex environments where the landscape is less structured, or features are sparse.

Despite the increase in APE, the improved trajectory alignment and reduced error throughout the entire path, as shown in the trajectory comparison, demonstrate the practical advantages of the proposed method. The integrated system outperforms AMCL in both APE and RPE metrics, offering improved localization consistency and long-term stability, which are vital for applications in agricultural environments where accuracy is essential for both short-term navigation and long-term operation.

VI. Conclusion

This paper introduces an integrated AMCL with NDT approach to enhance localization in agricultural environments. The method combines AMCL's efficiency in feature-sparse areas with the NDT's strength in structured environments, providing a robust solution for large-scale agricultural robotics. Although the integration leads to a slight increase in APE with the maximum APE rising by 60% (from 0.70 m to 1.12 m) and the mean APE increasing by 19.5% (from 0.41 m to 0.49 m)—it significantly improves RPE. Specifically, RPE Mean is reduced by 54.6% (from 1.12 m to 0.15 m), and RPE RMSE is reduced by 72.3% (from 1.46 m to 0.41 m). While the maximum APE is higher, the integrated approach results in

less error throughout the entire trajectory, offering improved consistency and stability. Despite the slight worsening of APE, the integrated method delivers enhanced localization consistency and long-term stability, which are crucial for agricultural applications. The method offers a cost-effective and reliable solution, effectively reducing drift and improving overall performance in large-scale agricultural fields.

Looking ahead, future research could explore the use of alternative scan matching algorithms alongside AMCL to further enhance localization accuracy in both feature-sparse and structured environments. Additionally, future tests in actual agricultural fields will be essential to validate the system's performance in real-world conditions, where dynamic factors such as changing terrain and environmental variables play a significant role in localization.

VII. Acknowledgment

This work was supported by Universiti Teknologi Malaysia (UTM) through UTM Fundamental Research (UTMFR) Grant (Q.K130000.3857.23H59) and UTM Matching Grant Q.K130000.3057.05M12).

References

[1] J. Lowenberg-Deboer and B. Erickson, "Precision agriculture for sustainability and productivity," *Agricultural Systems*, vol. 174, pp. 1–10, 2019.

[2] M. Fasiolo, D. Rossi, and P. Verdi, "Survey of localization techniques in precision agriculture," *Journal of Agricultural Robotics*, vol. 12, pp. 45–67, 2023.

[3] Z. He and J. Wang, "Environmental challenges for localization algorithms in agriculture," *Journal of Robotics*, vol. 34, pp. 78–89, 2017.

[4] L. Peng, M. Zhang, and X. Li, "An improved amcl algorithm based on laser scanning match in a complex and unstructured environment," *Advanced Robotics*, vol. 32, pp. 109–124, 2018.

[5] S. Thrun, D. Fox, and W. Burgard, "Monte carlo localization for mobile robots," *Robotics and Automation Systems*, vol. 23, pp. 99–110, 2000.

[6] Y. Chung and C. Lin, "An improved localization of mobile robotic system based on amcl algorithm," *Robotics Journal*, vol. 39, pp. 112–119, 2022.

[7] Z. He, Y. Li, and J. Wang, "Localization challenges in outdoor environments for autonomous robots," *Journal of Robotics Research*, vol. 45, pp. 345–362, 2023.

[8] H. Ren and X. Liu, "Large-scale outdoor slam based on 2d lidar," *Autonomous Robots*, vol. 42, pp. 211–229, 2019.

[9] Y. Liu and H. Zhang, "Improved localization algorithm for automatic guided vehicles," *Robotics Journal*, vol. 38, pp. 341–357, 2019.

[10] M. Yusuf, J. Smith, and R. Khan, "Cost-effective 2d lidar applications in agriculture," *Journal of Agricultural Robotics*, vol. 16, pp. 112–125, 2022.

[11] X. Peng *et al.*, "An improved amcl algorithm based on laser scanning match in a complex and unstructured environment," *Journal of Robotics Research*, vol. 35, pp. 123–135, 2018.

[12] X. Liu *et al.*, "Localization in outdoor environments using 2d lidar: Challenges and opportunities," *International Journal of Robotics*, vol. 40, pp. 95–110, 2023.

[13] J. He *et al.*, "Pose estimation challenges with amcl in unstructured outdoor environments," *Robotics and Autonomous Systems*, vol. 50, pp. 567–580, 2023.

[14] J. He and et al., "Challenges in pose estimation for mobile robots in symmetrical environments," *Advanced Robotics*, vol. 45, pp. 101–114, 2017.

[15] P. Biber and W. Straßer, "The normal distributions transform: A new approach to laser scan matching," in *Proceedings of the IEEE/RSJ International Conference on Intelligent Robots and Systems (IROS)*, 2003, pp. 2743–2748.

[16] M. Magnusson, A. Lilienthal, and T. Duckett, "Scan matching algorithms for mining environments: A comparative study," *Robotics and Autonomous Systems*, vol. 56, pp. 62–72, 2007.

[17] H. Sobreira, J. Silva, and A. Sousa, "Comparison of ndt and icp for localization in outdoor environments," *International Journal of Robotics Research*, vol. 38, pp. 1234–1248, 2019.

[18] H. Zhang, L. Wang, and Y. Xu, "Scalability challenges in icp and ndt for large-scale localization," *Autonomous Robots*, vol. 46, pp. 567–582, 2022.

[19] J. Sturm, N. Engelhard, F. Endres, W. Burgard, and D. Cremers, "A benchmark for the evaluation of rgb-d slam systems," in *Proceedings of the IEEE/RSJ International Conference on Intelligent Robots and Systems (IROS)*, 2012, pp. 573–580.

[20] B. K. Horn, "Closed-form solution of absolute orientation using unit quaternions," *Journal of the Optical Society of America A*, vol. 4, no. 4, pp. 629–642, 1987.